Macromolecules

Article

pubs.acs.org/Macromolecules

Comparative Study of Solution Properties of Amphiphilic 8-Shaped Cyclic-(Polystyrene-*b*-Poly(acrylic acid))$_2$ and Its Linear Precursor

Xu Wang,[†] Lianwei Li,*[,†] Xiaodong Ye,*[,†] and Chi Wu[†,‡]

[†]Hefei National Laboratory for Physical Sciences at the Microscale, Department of Chemical Physics, University of Science and Technology of China, Hefei, Anhui 230026, China

[‡]Department of Chemistry, The Chinese University of Hong Kong, Shatin N. T., Hong Kong

Supporting Information

ABSTRACT: Amphiphilic 8-shaped cyclic-(polystyrene-*b*-poly(acrylic acid))$_2$ with two rings and its linear precursor, i.e., 8-shaped cyclic- and linear-(PS−PAA)$_2$, were successfully prepared by a combination of atom transfer radical polymerization (ATRP) and "click" chemistry. Using various methods, we characterized those intermediates and resultant copolymers and studied their association properties in solutions. As expected, the average aggregation number ($\langle N_{agg} \rangle$) increases with the molar fraction of styrene for a given overall degree of polymerization. Our results reveal that the cyclization leads to a smaller $\langle N_{agg} \rangle$ but slightly larger and looser aggregates, presumably due to the topological constraint of the two rings (8-shaped). Using these amphiphilic chains as emulsifying agents, we found that 8-shaped cyclic-(PS−PAA)$_2$ chains are less effective in stabilizing latex particles in emulsion polymerization because each cyclic chain occupies a smaller interfacial surface area than its linear counterpart. Further, using pyrene as a model hydrophobic molecule, we investigated their solubilization powers. Our results reveal that 8-shaped cyclic- and linear-(PS−PAA)$_2$ chains have a similar ability in loading hydrophobic pyrene molecules, different from our original expectation, presumably because the hydrophobic PS block is too short and the hydrophilic PAA rings are too small. The current study provides a better understanding of the complicated topological constraint on the solution properties of 8-shaped cyclic amphiphilic copolymers.

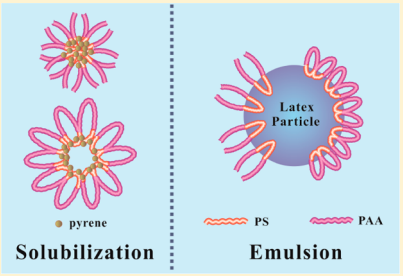

INTRODUCTION

Cyclic polymers have attracted much attention due to their unique solution and bulk properties in comparison with their linear analogues, such as a smaller hydrodynamic volume (V_h), a lower intrinsic viscosity ([η]), different phase transition temperatures in solutions, different melting (T_m), and glass-transition temperatures (T_g) in bulk.[1−5] Therefore, great efforts have been spent to synthesize homo- and hetero-single-cycle-shaped polymers.[4−19] Along this direction, other cycle-based polymers and copolymers with complicated topologies are also synthesized and studied, including tadpole-,[20−22] sun-,[23,24] and 8-shaped[22,25−33] polymers.

Among these complicated topologies, the 8-shaped structure might be the simplest one that contains two cycles connected by one point. Therefore, as a model, it has been used to explore the correlation between the structure and property for other more complicated cycle-based polymers and copolymers. Up to now, only few 8-shaped polymers with various compositions have been prepared. For example, Deffieux and Schappacher[33] prepared 8-shaped poly(chloroethyl vinyl ether) (PCEVE) by starting from a linear tetrafunctional precursor with two terminal acetal and two terminal styrenyl groups; Tezuka and co-workers[31,32] synthesized 8-shaped polytetrahydrofuran (PTHF)$_2$ and polystyrene (PS)$_2$ by using an electrostatic self-assembly and covalent fixation process; Jérôme et al.[30] synthesized 8-shaped poly(ε-caprolactone) (PCL)$_2$ via the controlled ring-expansion polymerization of lactones and the successive macrocyclization by the photo-cross-linking of pendant unsaturations; Pan and co-workers[27−29] prepared 8-shaped polymers composed of hydrophobic PS and PCL blocks via the "click" chemistry and studied their respective thermal and crystallization behaviors; and Wang and co-workers[25,26] prepared homo-poly(ethylene oxide) (PEG)$_2$ and hetero-8-shaped (PEG-*b*-PS)$_2$ polymers by a combination of atom transfer radical polymerization (ATRP), anionic ring-opening polymerization (ROP), and the "click" chemistry. Note that most of previous works were focused on different synthetic strategies and their cyclization efficiency with less attention on a systematical investigation of the solution properties of these 8-shaped polymers, especially those amphiphilic ones.

Linear amphiphilic copolymer chains,[34−36] especially those made of hydrophobic PS and hydrophilic poly(acrylic acid) (PAA),[37−41] have been extensively studied in the past few decades because of their various applications as emulsifiers, stabilization and flocculation agents, depending on their particular chain structures and lengths. Recently, we have comparatively studied the interchain association of a hyper-branched copolymer, hyper-(PAA−PS−PAA)$_n$, and its linear triblock PAA−PS−PAA precursor in dilute and semidilute solutions[42] and explored the solution properties of linear, cyclic,

Received: January 4, 2014
Revised: March 20, 2014
Published: March 27, 2014

dx.doi.org/10.1021/ma5000255 | *Macromolecules* 2014, 47, 2487−2495

and multiblock PS-*b*-PAA chains as surfactants in the emulsion polymerization.[43] Our results showed that the chain topology could significantly influence the solution properties of polymer chains in dilute and semidilute solutions.

In the current study, we further extended our investigation to the 8-shaped amphiphilic chains made of PAA and PS because we thought that each 8-shaped chain can lay itself flatly on an interface and cover a larger surface area than its linear precursor chain so that it might be a better emulsifier to stabilize more interfacial areas of latex particles for a given surfactant concentration. First, we prepared amphiphilic linear-$(PS-PAA)_2$ triblock copolymers and their cyclized 8-shaped copolymers, cyclic-$(PS-PAA)_2$, with two different styrene contents but a similar overall degree of polymerization by combining ATRP, "click" chemistry, and hydrolysis reaction, as shown in Scheme 1, where the initiator (**I**) preparation is

Scheme 1. Schematic of Synthesis of Linear- and 8-Shaped Cyclic-$(PS-PAA)_2$[a]

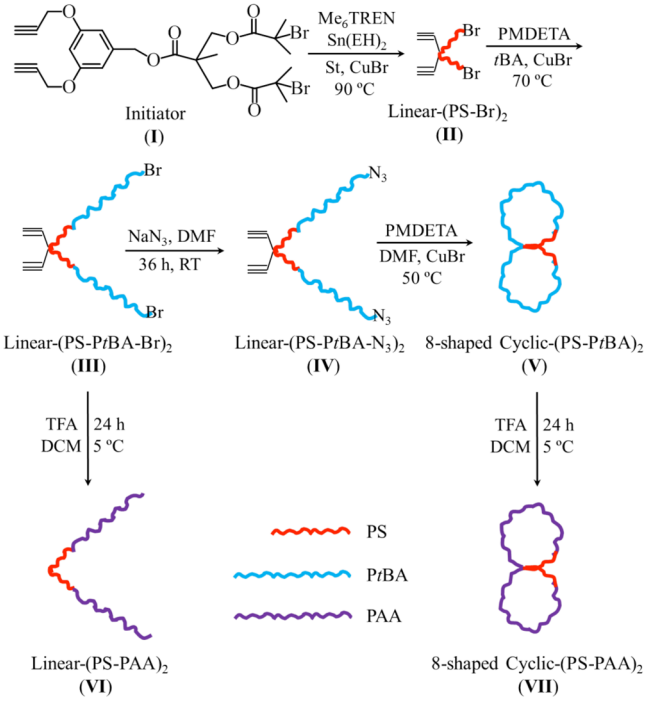

[a]St: styrene; Me_6TREN: tris(2-dimethylaminoethyl)amine; $Sn(EH)_2$: tin(II) 2-ethylhexanoate; *t*BA: *tert*-butyl acrylate; DMF: *N*,*N*-dimethylformamide; PMDETA: *N*,*N*,*N*′,*N*″,*N*″-pentamethyldiethylenetriamine; TFA: trifluoroacetic acid; DCM: dichloromethane.

detailed in the Supporting Information; then, characterized them by size exclusion chromatography (SEC), Fourier transform infrared spectroscopy (FT-IR), and proton nuclear magnetic resonance (^{1}H NMR) spectroscopy; and finally, studied their self-association in dilute aqueous solutions, their emulsifying efficiency in the emulsion polymerization of styrene, and their ability of dissolving hydrophobic chemicals in water by using laser light scattering (LLS), transmission electron microscopy (TEM), and ultraviolet−visible (UV−vis) spectroscopy.

EXPERIMENTAL SECTION

Materials. Styrene (St, Sinopharm, 97%) and *tert*-butyl acrylate (*t*BA, Sinopharm, 97%) were respectively passed through a basic alumina column to remove the inhibitor and then distilled under a reduced pressure over CaH_2. Copper(I) bromide (CuBr, Alfa, 98%) was washed with glacial acetic acid to remove soluble oxidized species, filtrated, then further washed with ethanol, and dried under vacuum. *N*,*N*-Dimethylformamide (DMF, Sinopharm, AR) was distilled under a reduced pressure over $MgSO_4$, and tetrahydrofuran (THF, Alfa, 99%) was refluxed over sodium for 24 h and distilled prior to use. Milli-Q water with a resistivity of 18.2 MΩ·cm was used. Other reagents were used as received without further purification.

The synthesis of linear- and 8-shape cyclic-$(PS_{14}-PAA_{17})_2$ is detailed as follows, and the syntheses of linear- and 8-shaped cyclic-$(PS_8-PtBA_{26})_2$ are similar and can be found in the Supporting Information.

Synthesis of Linear-$(PS_{14}$-Br$)_2$. A reaction flask equipped with a magnetic stirrer and a rubber septum was charged with 0.50 g of initiator (**I**) (0.793 mmol), 4.13 g of styrene (39.7 mmol), 91.0 mg of tris(2-dimethylaminoethyl)amine (Me_6TREN) (0.40 mmol), and 0.16 g of tin(II) 2-ethylhexanoate ($Sn(EH)_2$) (0.40 mmol). The flask was degassed by three freeze−pump−thaw cycles, backfilled with N_2, and then placed in an oil bath thermostated at 90 °C. After ∼2 min, 11.5 mg of CuBr (0.079 mmol) was introduced to start the polymerization. After the reaction, the flask was rapidly cooled to room temperature. The polymer mixture was diluted with THF and then passed through a short column of neutral alumina to remove metal salts. After the solvent was removed by evaporation, the residue was dissolved in THF and precipitated into an excess amount of methanol. The purification process was repeated twice. Linear-$(PS_{14}-Br)_2$ was obtained (2.10 g, yield: 45.3%) after drying in vacuum overnight at 45 °C.

Synthesis of Linear-$(PS_{14}-PtBA_{17}$-Br$)_2$. A reaction flask equipped with a magnetic stirrer and a rubber septum was charged with 1.50 g of linear-$(PS_{14}$-Br$)_2$ (0.423 mmol), 5.40 g of *t*BA (42.3 mmol), 24.4 mg of *N*,*N*,*N*′,*N*″,*N*″-pentamethyldiethylenetriamine (PMDETA) (0.140 mmol), and 1.4 mL of dry acetone. The flask was degassed by three freeze−pump−thaw cycles, backfilled with N_2, and then placed in an oil bath thermostated at 70 °C. After ∼2 min, 20.2 mg of CuBr (0.140 mmol) was introduced to start the polymerization. After the reaction, the flask was cooled to room temperature. The polymer mixture was diluted with THF and then passed through a short column of neutral alumina to remove metal salts. After the solvent was removed by a rotary evaporator, the residue was dissolved in a small amount of THF and precipitated into an excess amount of cold methanol/water mixture (3/1, v/v). The above purification process was repeated twice. Linear-$(PS_{14}-PtBA_{17}$-Br$)_2$ was obtained (2.30 g, yield: 33.3%) after drying in a vacuum oven overnight at 45 °C.

Synthesis of Linear-$(PS_{14}-PtBA_{17}$-$N_3)_2$. A 30 mL round-bottom flask was charged with 1.20 g of linear-$(PS_{14}-PtBA_{17}$-Br$)_2$ (0.152 mmol), 15.0 mL of DMF, and 98.8 mg of NaN_3 (1.52 mmol). The mixture was stirred at room temperature for 36 h. After most of the solvent was removed under a reduced pressure, the remaining solution was diluted with dichloromethane (DCM) and then precipitated into an excess amount of cold methanol/water mixture (3/1, v/v). The sediments were redissolved in DCM, passed through a neutral alumina column to remove residual sodium salts, and then precipitated into an excess amount of cold methanol/water mixture (3/1, v/v). Linear-$(PS_{14}-PtBA_{17}$-$N_3)_2$ was obtained (1.10 g, yield 91.7%) after drying in a vacuum oven overnight at 45 °C.

Synthesis of Cyclic-$(PS_{14}-PtBA_{17})_2$. 1.5 L of DMF was added into a 2 L round-bottom flask and bubbled with N_2 for 10 h. 1.00 g of CuBr (7.0 mmol) and 1.20 g of PMDETA (7.0 mmol) were introduced. The degassed 1.00 g of precursor linear-$(PS_{14}-PtBA_{17}$-$N_3)_2$ (0.127 mmol) in 50.0 mL of DMF was added to the CuBr/PMDETA complex DMF solution at 50 °C via a syringe pump at a rate of 0.8 mL/h. After adding the polymer solution, the reaction was allowed to proceed for another 2 h. The mixture was then cooled to room temperature, concentrated in vacuum, and then diluted with 200 mL of DCM. The organic layer was washed twice using a saturated sodium bisulfate ($NaHSO_4$) solution to remove most of the metal catalyst, dried over anhydrous magnesium sulfate ($MgSO_4$), and filtered through neutral alumina to remove trace metal catalyst. After

dx.doi.org/10.1021/ma5000255 | *Macromolecules* 2014, 47, 2487−2495

most of the solvent was removed by a rotary evaporator, the residue was precipitated into cold methanol/water mixture (3/1, v/v). After drying in a vacuum oven overnight at 45 °C, cyclic-$(PS_{14}-PtBA_{17})_2$ was obtained.

Purification of Cyclic-$(PS_{14}-PtBA_{17})_2$. Cyclic-$(PS_{14}-PtBA_{17})_2$ was dissolved in THF at room temperature with a concentration of ~0.04 g/mL in a round-bottom flask. A mixture of methanol/water (3/1, v/v) was slowly dropped into the polymer THF solution until the solution became slightly milky. The temperature controlled by a water bath with a precision of ±0.1 °C was raised until the solution became clear again. Then the solution was slowly cooled until it became slightly milky, and the solution temperature was maintained to allow a very small fraction of longest polymer chains to precipitate. A small amount of precipitate (~10 wt %) was removed. The purification process was repeated twice. The upper clear solution was recycled by a rotary evaporator to give pure cyclic product without detectable multiblock impurity (0.77 g, yield 77.0%).

Hydrolysis of Linear- and Cyclic-$(PS_{14}-PtBA_{17})_2$. Linear-$(PS_{14}-PtBA_{17})_2$ was dissolved in DCM with a concentration of ~50.0 g/L and a 5-fold molar excess of trifluoroacetic acid (TFA) with respect to the *tert*-butyl groups in the copolymer was added under nitrogen atmosphere at 5 °C to avoid the possible cleavage of the benzyl ester. After 24 h, TFA and DCM were removed by a rotary evaporator. The collected polymer was dissolved in THF/water (1/1, v/v), transferred into presoaked dialysis tubing with a molecular weight cutoff (MWCO) value of 3000 Da, and then dialyzed against deionized water for 5 days. After the freeze-drying process, a fluffy white solid linear-$(PS_{14}-PAA_{17})_2$ (0.80 g) was obtained. Cyclic-$(PS_{14}-PAA_{17})_2$ (0.60 g) was obtained by a similar procedure.

Preparation of Polymer Solutions. Linear- and cyclic-$(PS_8-PAA_{26})_2$ chains were directly dissolved in an aqueous solution containing 40 mM Na_2CO_3 and 100 mM NaCl at 70 °C and stirred for 30 min. Linear- and cyclic-$(PS_{14}-PAA_{17})_2$ with a long hydrophobic PS block were first dissolved in 1 mL of THF, and then the THF solution was slowly injected into an aqueous solution containing 40 mM Na_2CO_3 and 100 mM NaCl within 1 h by a programmed syringe pump. The solvent THF was removed by evaporation under a reduced pressure at ~30 °C. To make up the water loss in the evaporation process, Milli-Q water was added to maintain the stock solution with a concentration of 2.0 g/L.

Emulsion Polymerization. The emulsion polymerization was performed in a 50 mL three-neck round-bottom flask immersed in a thermostated oil bath and equipped with a reflux condenser, a nitrogen inlet, and a thermometer. 27.0 mL of the micelle solution with different concentrations of linear- and cyclic-$(PS-PAA)_2$ was bubbled with nitrogen for 20 min at room temperature. Ten minutes after adding 3.0 g of styrene, an aqueous solution of initiator (39.0 mg of $K_2S_2O_8$, dissolved in 3 mL of degassed deionized water) was introduced to start the polymerization. The emulsion polymerizations were conducted at 70 °C. The pH of the reaction mixture was kept ~9.0 to ensure full ionization of the carboxylic acid groups. The reactions were carried for 4 h to ensure complete conversion.

Latex Characterization. The particle morphology, polymer solid content (τ), and average hydrodynamic radius ($\langle R \rangle$) of such prepared latexes were characterized by TEM, gravimetry, and dynamic LLS in HCl aqueous solution (pH ~ 3.1), respectively. The latex particle number density (N_p) was calculated according to

$$N_p = \frac{3\tau}{4\pi\rho\langle R\rangle^3} \tag{1}$$

where ρ is the density of PS (ρ = 1.05 g/mL).[41]

Solubilization of Pyrene. Prior to the loading, pyrene was dissolved in anhydrous acetone with a concentration of 20.0 g/L. 0.1 mL of such a pyrene acetone solution was added into an empty vial and allowed to evaporate overnight to form a thin pyrene film on the wall. The quantity of pyrene (~2 mg) was at least 100 times in excess of the saturation limit for the highest polymer concentration. The polymer solutions were added into the vials and vigorously stirred first at 50 °C for 12 h and then at ~25 °C for another 12 h to ensure that the partitioning of pyrene between water and polymer phases has reached equilibrium, which is detailed in the Supporting Information. The excess of pyrene was removed by a 0.45 μm PTFE filter before UV–vis measurement. The concentrations of pyrene in polymer solutions ($C_{py,s}$) were calculated by the Lambert–Beer law, $A_{py,s} = \varepsilon b C_{py,s}$, with $A_{py,s}$, ε (~36 000 M^{-1} cm^{-1}), and b (= 1.0 cm) the absorbance of pyrene in the polymer solution with the subtraction of the absorbance due to PS–PAA polymer, the molar extinction coefficient of pyrene in polymer solutions, and the sample cell thickness. The measurement of the extinction coefficient (ε) of pyrene in polymer solutions at a wavelength of 340 nm is detailed in the Supporting Information.

Size Exclusion Chromatography (SEC). Relative number-average molar masses (M_n) and distributions (M_w/M_n) were determined by a size exclusion chromatography (SEC, Waters 1515) equipped with three Waters Styragel columns (HR2, HR4, and HR6) and a refractive index detector (RI, Wyatt WREX-02) at 35 °C. THF at a flow rate of 1.0 mL/min was used as the eluent, and a series of narrowly distributed polystyrene were used as standards.

Fourier Transform Infrared (FTIR) Spectroscopy. The FT-IR spectra were recorded on a NICOLET 8700 FTIR spectrometer. The spectra were collected over 64 scans with a spectral resolution of 4 cm^{-1}.

Laser Light Scattering (LLS). A commercial LLS spectrometer (ALV/DLS/SLS-5022F) equipped with a multidigital time correlator (ALV5000) and a cylindrical 22 mW UNIPHASE He–Ne laser (λ_0 = 632.8 nm) as the light source was employed for dynamic and static LLS measurements. In static LLS, the angular dependence of the absolute excess time-average scattering intensity, the Rayleigh ratio $R_{vv}(q)$, can lead to the weight-average molar mass (M_w), the root-mean-square gyration radius $\langle R_g^2 \rangle_z^{1/2}$ (or simply written as $\langle R_g \rangle$), and the second virial coefficient A_2 by using

$$\frac{KC}{R_{vv}(q)} \approx \frac{1}{M_w}\left(1 + \frac{1}{3}\langle R_g^2\rangle_z q^2\right) + 2A_2C \tag{2}$$

where $K = 4\pi^2 n^2 (dn/dC)^2/(N_A\lambda_0^4)$ and $q = (4\pi/\lambda_0)\sin(\theta/2)$ with C, dn/dC, N_A, and λ_0 the concentration of the polymer solution, the specific refractive index increment, Avogadro's number, and the wavelength of light in a vacuum. In dynamic LLS,[44] scattered light was collected at a fixed angle of 90° for a duration of 600 s. The average hydrodynamic radius ($\langle R_h \rangle$) and distribution ($f(R_h)$) were obtained using cumulants analysis and CONTIN routines. In static LLS,[45] the scattering intensity was recorded at each angle three times and was averaged over 10 s for each time, and the relative error was set within ±5%. The scattering angle ranged from 30° to 150°. The refractive index increments (dn/dC) of the $(PS_8-PAA_{26})_2$ and $(PS_{14}-PAA_{17})_2$ chains in aqueous solutions containing 40 mM Na_2CO_3 and 100 mM NaCl determined with a precise differential refractometer[46] were 0.130 and 0.156 mL/g, respectively.

Transmission Electron Microscopy (TEM). Latex particle morphology was measured on a transmission electron microscopy (TEM, JEOL JEM-2100). Before the TEM observation, each latex was directly diluted to a final concentration of ~50 ppm, and then a drop was placed on a carbon-coated copper grid and dried at 40 °C in a desiccator.

RESULTS AND DISCUSSION

Scheme 1 and Figure S1 show the synthetic process of amphiphilic linear and 8-shaped cyclic copolymers, linear-$(PS-PAA)_2$ and cyclic-$(PS-PAA)_2$, including synthesis of (1) the initiator (**I**) with two alkyne and two bromine groups; (2) linear precursors linear-$(PS\text{-}PtBA\text{-}N_3)_2$ (**IV**) by successive ATRP and azidation of bromide groups; (3) cyclic-$(PS\text{-}PtBA)_2$ (**V**) by intrachain "click" cyclization; and (4) linear- and cyclic-$(PS-PAA)_2$ (**VI** and **VII**) chains by hydrolysis reaction with TFA. The purity of the tetrafunctional initiator (**I**) with two alkyne and two bromine groups was verified by ^1H NMR, as shown in Figure 1A. Namely, the obtained area (A)

dx.doi.org/10.1021/ma5000255 | Macromolecules 2014, 47, 2487–2495

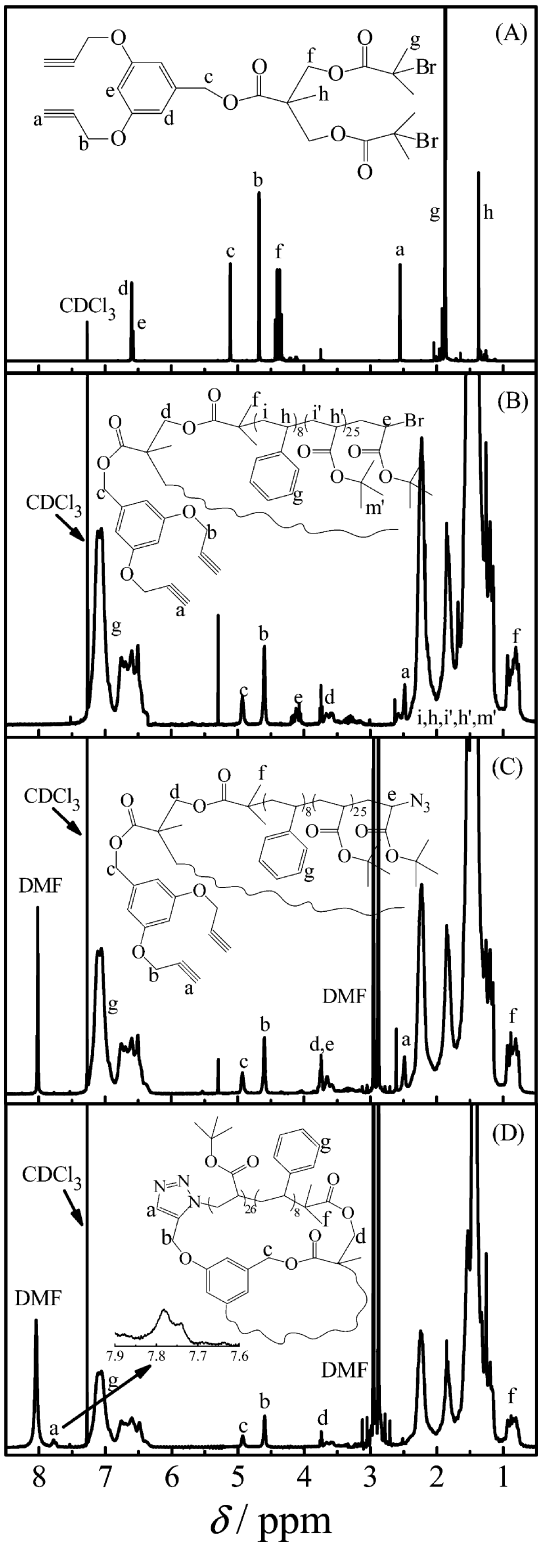

Figure 1. ^{1}H NMR spectra of (A) tetrafunctional initiator (**I**), (B) linear-$(PS_8-PtBA_{26}-Br)_2$ precursor, (C) linear-$(PS_8-PtBA_{26}-N_3)_2$, and (D) 8-shaped cyclic-$(PS_8-PtBA_{26})_2$. Solvent: $CDCl_3$.

ratio of the peak (*f*) to peak (*b*) is 0.98/1.00, close to the theoretical ratio. The preparation details and chemical characterization of the intermediates are shown in the Supporting Information (Figures S2–S4). Using the initiator **I** and ATRP, we prepared linear-$(PS_8-PtBA_{26})_2$ and linear-$(PS_{14}-PtBA_{17})_2$ with two different styrene molar contents but a similar overall degree of polymerization (*DP*).

In the current study, we have adopted activators regenerated by the electron transfer for atom transfer radical polymerization (ARGET ATRP) in the polymerization of styrene and reduced the CuBr concentration in the polymerization of *tert*-butyl acrylate, significantly suppressing the side reactions induced by the outer-sphere electron-transfer (OSET) and improving the chain-end functionality of linear-(PS-P*t*BA-Br)$_2$.[47−50]

The *DP* of the PS block was calculated from the area ratio of peaks *g* to *c* in the ^{1}H NMR spectrum after ignoring the small contribution of the protons of benzene in the initiator, as shown in Figure 1B.

$$DP_{PS} = (2A_g)/(5A_c) \tag{3}$$

The overlapping signals of peaks *i*, *h*, *i*′, *h*′, and *m*′ are contributed by methyl, methine, and methylene groups from both PS block and P*t*BA block. After knowing the *DP* of the PS block, we know the contribution of methine and methylene groups from the PS block so that the rest area is only contributed from methyl, methine, and methylene groups of P*t*BA block. Therefore, the *DP* of the P*t*BA block was calculated from the area ratio of peaks *i*, *h*, *i*′, *h*′, *m*′ to peak *g* as

$$DP_{PtBA} = DP_{PS}\frac{5A_{i,h,i',h',m'} - 3A_g}{12A_g} \tag{4}$$

After obtaining well-defined triblock linear-$(PS_8-PtBA_{26}-Br)_2$ and linear-$(PS_{14}-PtBA_{17}-Br)_2$ with a high chain-end functionality, we replaced each bromine with an azide group in DMF by an efficient substitution reaction, which was confirmed by ^{1}H NMR and IR spectra. Namely, as shown in Figures 1B and 1C, the signal of the proton located at the chain end changes from ∼4.10 ppm (proton *e* in Figure 1B) to ∼3.60 ppm (proton *e* in Figure 1C). The replacement of the bromine with the azide group was also reflected in the presence of a strong N═N═N antisymmetric stretch vibration absorption band near ∼2100 cm^{-1}, as shown in Figure 2B.

To suppress the interchain coupling, the cyclization of individual linear-(PS-P*t*BA-N_3)$_2$ chains via the "click" reaction was carried by slowly adding the copolymer solution into a DMF solution with an excess amount of CuBr/PMDETA

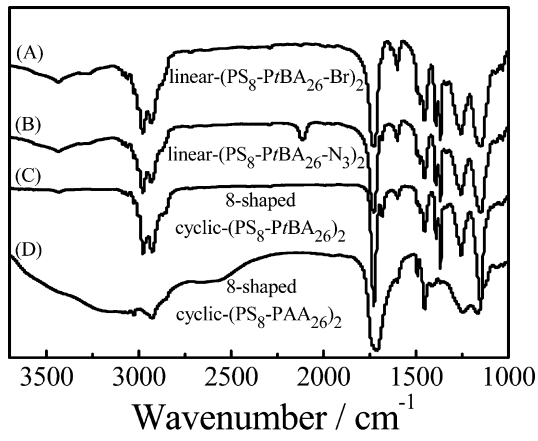

Figure 2. IR spectra of (A) linear-$(PS_8-PtBA_{26}-Br)_2$, (B) linear-$(PS_8-PtBA_{26}-N_3)_2$, (C) 8-shaped cyclic-$(PS_8-PtBA_{26})_2$, and (D) 8-shaped cyclic-$(PS_8-PAA_{26})_2$.

dx.doi.org/10.1021/ma5000255 | *Macromolecules* 2014, 47, 2487−2495

catalyst to ensure the high "clicking" efficiency. Figure 3 and Table 1 summarize the SEC characterization results of all the

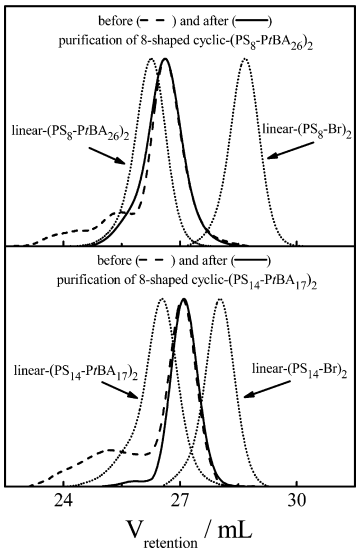

Figure 3. SEC curves of different copolymers before and after purification. Temperature: 35 °C. Eluent: THF at a flow rate of 1.0 mL/min. Standards: narrowly distributed polystyrenes.

Table 1. Summary of SEC Characterization of Different (PS−P*t*BA)$_2$ Copolymers

copolymer	M_n[a] (g/mol)	M_p[b] (g/mol)	M_w/M_n[a]	$M_{p,cyclic}/M_{p,linear}$
linear-(PS$_8$−P*t*BA$_{26}$)$_2$	8.8 × 10^3	9.1 × 10^3	1.10	0.79
cyclic-(PS$_8$−P*t*BA$_{26}$)$_2$	7.1 × 10^3	7.2 × 10^3	1.15	
linear-(PS$_{14}$−P*t*BA$_{17}$)$_2$	7.8 × 10^3	7.8 × 10^3	1.12	0.75
cyclic-(PS$_{14}$−P*t*BA$_{17}$)$_2$	5.6 × 10^3	5.8 × 10^3	1.10	

[a] M_n and M_w/M_n were obtained by using polystyrene standards in SEC. [b] M_p is the molar mass of the elution peak in SEC curve.

polymers, which reveal that such prepared linear-(PS-Br)$_2$ and linear-(PS-P*t*BA-Br)$_2$ chains are narrowly distributed with a polydispersity index (M_w/M_n) of ~1.15. However, for the crude polymers after the cyclization, there exists an obvious tail at a smaller retention volume, signaling the interchain coupling. The linear and/or cyclic multiblock copolymers (10−20 wt %) as byproducts were further removed by the precipitation fractionation. It should be stated that there might still exist a trace amount of undetectable noncyclized linear chains, but they will not noticeably influence the solution properties of cyclic copolymer chains.

The ratios listed in the last column of Table 1 were calculated from the peak values of the molar masses of cyclic and linear copolymer ($M_{p,cyclic}$ and $M_{p,linear}$) in the SEC curves. Figure 3 shows that in the SEC curves the peak of cyclic copolymers shifts to the longer retention time, and the ratios of $M_{p,cyclic}/M_{p,linear}$ become 0.79 and 0.75, respectively, agreeing well with previously observed ones.[22,25−30,33] Moreover, the signal of methine proton (~2.5 ppm) located at the chain end disappears (Figure 1C), and a new signal of triazine (7.6−7.8 ppm) appears after the cyclization (Figure 1D); similarly, the disappearance of the N═N═N antisymmetric stretch peak near ~2100 cm^{-1} also reflects that the "click" reaction is complete (Figure 2C).

Further TFA hydrolysis of the *tert*-butyl groups into the carboxyl acid groups leads to the corresponding well-defined amphiphilic cyclic-(PS−PAA)$_2$ and linear-(PS−PAA)$_2$ chains, reflecting in the broad carboxylic acid −OH bond stretching peak (3700−2700 cm^{-1}) (Figure 2D). The typical degree of hydrolysis by TFA is over 90% according to the literature.[51] The ^{1}H NMR spectra of linear PS-P*t*BA copolymer before and after the hydrolysis show that the degree of hydrolysis is nearly complete (>99%), as further discussed in the Supporting Information (Figure S5). Note that the stability of ester groups to acid is in the following order: benzyl > methyl > *t*-butyl, and benzyl ester is stable even at pH = 1 at room temperature.[52] Furthermore, controlled experiments detailed in the Supporting Information (Figure S5) were carried out to study the stability of benzyl esters in the novel initiator, and the results show that the benzyl ester was intact during the TFA hydrolysis process, which is expected because the deprotection of the benzyl ester is generally selectively catalyzed by palladium under a hydrogen atmosphere.[53] Using the above synthetic strategy, we finally obtained two sets of amphiphilic linear- and cyclic-(PS−PAA)$_2$ chains with different styrene molar fractions but a similar overall degree of polymerization ($DP \sim 65$).

For studying the association of linear- and cyclic-(PS−PAA)$_2$ in water, we added 100 mM NaCl and 40 mM Na_2CO_3 in the aqueous solutions to reduce the polyelectrolytes effect and dissociate all the carboxylic acid groups (−COOH) into carboxylic anions (−COO$^-$ + H$^+$).[40,41] As mentioned before, linear- and cyclic-(PS$_8$−PAA$_{26}$)$_2$ chains with a short hydrophobic PS block were readily soluble in the aqueous solutions. Thus, they were directly dissolved in an aqueous solution containing 40 mM Na_2CO_3 and 100 mM NaCl at 70 °C and stirred for 30 min. However, linear- and cyclic-(PS$_{14}$−PAA$_{17}$)$_2$ with a long hydrophobic PS block cannot be dissolved in aqueous solutions directly. They were first dissolved in 1 mL of THF, and then the THF solution was slowly injected into an aqueous solution containing 40 mM Na_2CO_3 and 100 mM NaCl within 1 h by a programmed syringe pump. Such prepared four copolymer solutions (more precisely, dispersions) were characterized by LLS. The results are shown in Figures 4 and 5.

In Figure 4, $KC/R_{vv}(q)$ at $q \to 0$ is related to the reciprocal of the weight-averaged molar mass of the scattering objects ($1/M_w$) if we ignore a small concentration correction for a dilute solution or dispersion as described in eq 2. It is clear that both

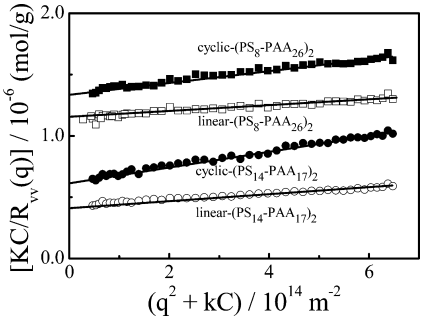

Figure 4. Scattering vector (q) dependence of Rayleigh ratio ($R_{vv}(q)$) of different linear- and 8-shaped cyclic-(PS−PAA)$_2$ in aqueous solutions with 40 mM Na_2CO_3 and 100 mM NaCl, where $C_{polymer}$ = 2.0 g/L.

dx.doi.org/10.1021/ma5000255 | *Macromolecules* 2014, 47, 2487−2495

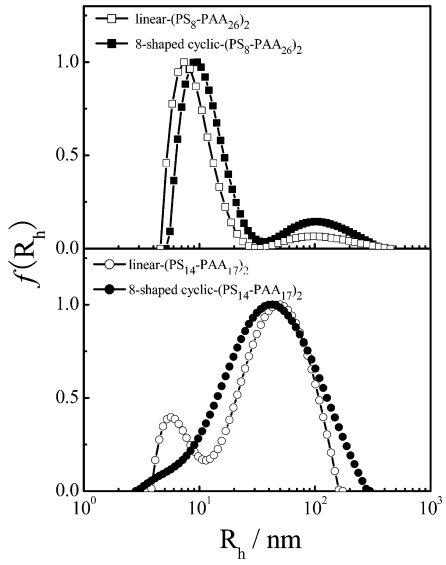

Figure 5. Hydrodynamic radius distributions ($f(R_h)$) of (A) linear- and 8-shaped cyclic chains with a shorter PS block and (B) linear- and 8-shaped cyclic chains with a longer PS block in aqueous solutions with 40 mM Na_2CO_3 and 100 mM NaCl, where $C_{polymer}$ = 2.0 g/L.

the chain topology and the hydrophobic PS block length affect the chain association in the aqueous solution, reflecting in different weight-average aggregation numbers ($\langle N_{agg}\rangle$), defined as $\langle N_{agg}\rangle = M_{w,agg}/M_{w,chain}$, where $M_{w,agg}$ is the apparent weight-average molar mass of aggregates and $M_{w,chain}$ is the weight-average molar mass of each individual chain. As expected, $\langle N_{agg}\rangle$ increases with the molar fraction of styrene for a given topology. It is interesting to see that for a given molar fraction of styrene linear chains have larger $\langle N_{agg}\rangle$ than their cyclic analogues. In other words, linear chains have a more tendency to associate in the aqueous solution than their cyclic counterparts. Literature search shows that only few experimental results were reported about the topology-dependent aggregation properties.[6] Recently, Tezuka and co-workers comparatively studied the association of amphiphilic cyclic-poly(methyl acrylate)-*b*-poly(ethylene oxide) and their linear analogues in water and reported the topology effects on the properties of linear and cyclized polymeric amphiphiles. Their static light scattering measurements showed that linear PMA-*b*-PEO-*b*-PMA have larger $\langle N_{agg}\rangle$ values compared with cyclic-PMA-*b*-PEO,[6,13] which is consistent with our results. Our current results in Figure 4 reveal that the interchain association is moderately suppressed by topological constraint of the double cycles in the 8-shaped chains. One can image that as more cycles were interconnected, most of those hydrophobic segments would be wrapped inside so that their interchain association would be suppressed and the intrachain association of those hydrophobic segments would even lead to the formation of single chain micelles in the aqueous solution.

In dynamic LLS, Figure 5 shows that there are two peaks, respectively located at ~10 and ~90 nm, for both linear- and cyclic-$(PS_8-PAA_{26})_2$, indicating the formation of small and large interchain aggregates. In contrast, for both linear- and cyclic-$(PS_{14}-PAA_{17})_2$ chains with a longer hydrophobic PS block, there is a large peak located at ~50 nm. Note that the contour length of a fully stretched $PS_{14}-PAA_{17}$ chain is only ~8 nm, much smaller than ~50 nm, indicating that such a peak is due to the formation of some irregular interchain association, not small well-defined core−shell micelles, presumably because of the stronger hydrophobic interaction among the longer PS blocks. Similar phenomena were reported for other systems, especially for those hydrophobic blocks with a high glass transition temperature (T_g) and high interfacial energy.[25,54,55] We also find that the aggregates made of 8-shaped cyclic chains have a smaller $\langle N_{agg}\rangle$ but a larger $\langle R_h\rangle$ (Table 2), indicating that

Table 2. LLS Characterization of Linear- and 8-Shaped Cyclic-(PS-PAA)$_2$ in Aqueous Solutions Containing 40 mM Na_2CO_3 and 100 mM NaCl

copolymer	$M_{w,agg}$ (g/mol)	$\langle N_{agg}\rangle^a$	$\langle R_h\rangle^b$ (nm)	$\mu_2/\langle D\rangle^{2\,c}$
linear-$(PS_8-PAA_{26})_2$	8.8×10^5	147	11	0.19
cyclic-$(PS_8-PAA_{26})_2$	7.3×10^5	122	14	0.20
linear-$(PS_{14}-PAA_{17})_2$	2.2×10^6	367	35	0.22
cyclic-$(PS_{14}-PAA_{17})_2$	1.5×10^6	250	46	0.24

$^a N_{agg} = M_{w,agg}/M_{w,chain}$, where $M_{w,chain}$ is 6.0×10^3 g/mol. ^{b}Measured by dynamic LLS at 90°. ^{c}In which μ_2 stands for relative line width of diffusion coefficient distribution and $\langle D\rangle$ stands for average diffusion coefficient.

they have a looser structure in comparison with those made of their linear analogues. Scheme 2 illustrates the aggregates of linear- and 8-shaped cyclic-$(PS-PAA)_2$ formed in aqueous solutions.

Scheme 2. Schematic of the Aggregates of Linear- and 8-Shaped Cyclic-(PS−PAA)$_2$ Formed in Aqueous Solutions

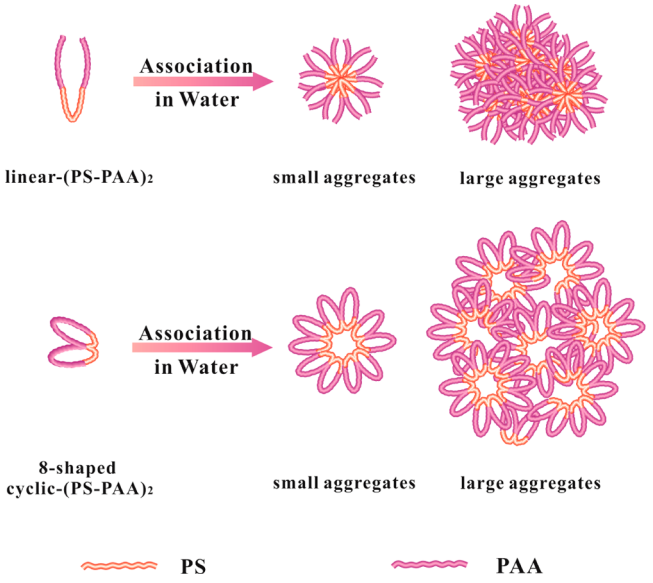

The amphiphilic nature of these copolymers leads to one of their main applications as polymeric surfactants to reduce the interfacial tension in the formation of latex particles in aqueous solutions and in the blending of two incompatible polymers, where the hydrophobic blocks anchor into one phase while the hydrophilic blocks extend into another one. Therefore, after studying their self-association in aqueous solutions, we used them to further explore how the chain topology affected the emulsifying ability in the formation of PS latex particles.

Figure 6 reveals that the latex particles stabilized by linear and cyclic surfactants are both spherical and narrowly dispersed, indicating that the copolymer topology has nearly no effect on the morphology and size distribution of the resultant latex

dx.doi.org/10.1021/ma5000255 | Macromolecules 2014, 47, 2487−2495

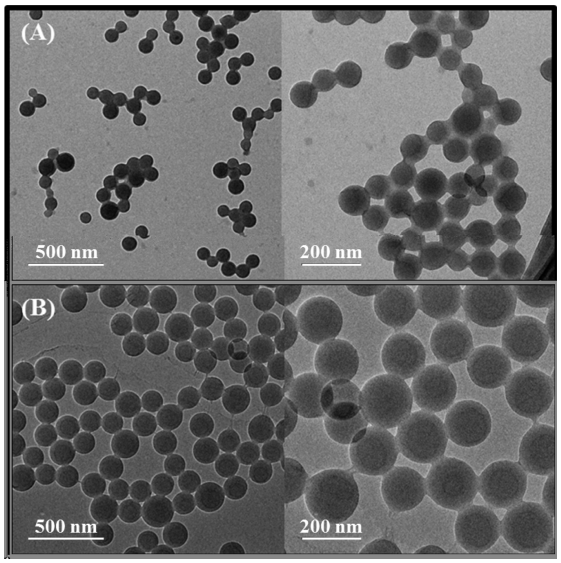

Figure 6. TEM characterization of the latex particles stabilized by (A) linear-$(PS_8-PAA_{26})_2$ and (B) 8-shaped cyclic-$(PS_8-PAA_{26})_2$, where $C_{polymer}$ = 0.5 g/L.

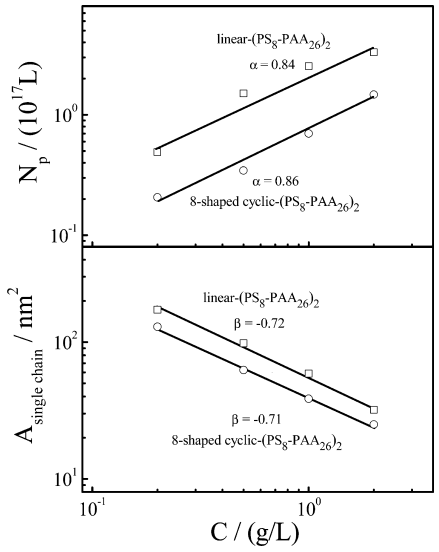

Figure 7. Amphiphilic copolymer concentration (C) dependence of average number density (N_p) and interfacial surface area ($A_{single\ chain}$) occupied per chain of polystyrene latex particles.

particles. However, it is obvious that the latex particles formed and stabilized by cyclic-$(PS_8-PAA_{26})_2$ chains are much larger than those formed and stabilized by linear-$(PS_8-PAA_{26})_2$ for a given copolymer concentration, indicating that each linear chain can stabilize more interfacial surface area ($A_{single\ chain}$) than its cyclic counterpart, where $A_{single\ chain}$ is defined as

$$A_{single\ chain} = \frac{A_{total}}{N_A C/M} \tag{5}$$

with N_A, C, M, and A_{total} the Avogadro number, the copolymer concentration, the copolymer molar mass, and the total interfacial surface areas of all the latex particles in the dispersion. A_{total} is further related to the number density (N_p) and radius ($\langle R \rangle$) of the latex particles as

$$A_{total} = 4\pi \langle R \rangle^2 N_p \tag{6}$$

A combination of eqs 1, 5, and 6 leads to

$$A_{single\ chain} = \frac{4\pi \langle R \rangle^2 N_p M}{N_A C} = \frac{3\tau M}{N_A \rho \langle R \rangle C} \tag{7}$$

On the other hand, one classic method for elucidating the effect of the initial concentration of surfactant molecules on both the resultant latex particle number density (N_p) and size ($\langle R \rangle$) shows that both N_p and $\langle R \rangle$ are scaled to C as[41]

$$N_p \sim C^{\alpha} \quad \text{or} \quad \langle R \rangle \sim C^{-\alpha/3} \tag{8}$$

A further combination of eqs 7 and 8 results in

$$A_{single\ chain} \sim C^{\beta} \quad \text{and} \quad \beta = \alpha/3 - 1 \tag{9}$$

Figure 7 shows that linear- and cyclic-$(PS_8-PAA_{26})_2$ chains as polymeric surfactants lead to similar scaling exponents of α and β, indicating that they have similar unimer extraction and diffusion. However, 8-shaped cyclic-$(PS_8-PAA_{26})_2$ chains lead to a lower N_p and a smaller $A_{single\ chain}$, similar to the results of circular PAA–PS chains.[43] Originally, we thought that 8-shaped cyclic chains with two rings could flatly lay on the interface to stabilize more surface area but forgot that the formation of two small PAA rings restricts the chain extension so that they actually cover a smaller surface area of the PS latex particle than two dangling PAA chains. Therefore, it would be better if one could make longer hydrophilic PAA chains, i.e., larger rings, but one has to solve the anchoring problem. The emulsion polymerization conditions are detailed in Table S1 in the Supporting Information.

Another application of amphiphilic copolymers is to carry biologically active ingredients, such as water-insoluble anticancer drugs.[56−60] To investigate the effect of chain topology on such an application, we chose pyrene as a model compound to explore the solubilization capacity of our amphiphilic linear- and cyclic-$(PS-PAA)_2$ in water. As shown in Figure 8, the

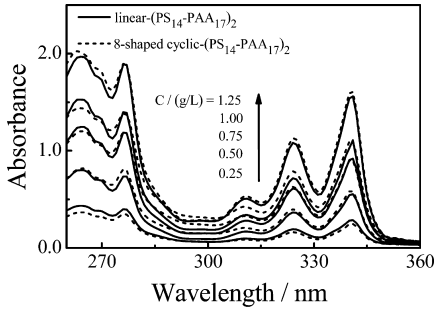

Figure 8. UV–vis spectra of pyrene solution solubilized by different amounts of amphiphilic linear- and 8-shaped cyclic-$(PS_{14}-PAA_{17})_2$.

typical UV–vis spectra of pyrene solutions show two characteristic absorbance peaks located at 324 and 340 nm, respectively, which were away from the absorbance bands of PS and PAA. It has been known that the maximum absorption wavelength of pyrene in pure water is ~334 nm[61] but shifts to a longer wavelength when pyrene is solubilized in the hydrophobic region of polymeric micelles.[62−65] In the current work, the peak is shifted to ~340 nm in the presence of PS–PAA copolymers and becomes higher as the copolymer concentration increases.

For comparison, the solubilization capacity of linear- and cyclic-$(PS-PAA)_2$ for pyrene in polymer aqueous solutions

dx.doi.org/10.1021/ma5000255 | Macromolecules 2014, 47, 2487−2495

($C_{py,s}/C_{py,w}$) is shown in Figure 9, where $C_{py,s}$ and $C_{py,w}$ (= 6.0 × 10^{-7} M at 25 °C[61,64]) are the pyrene concentrations with and

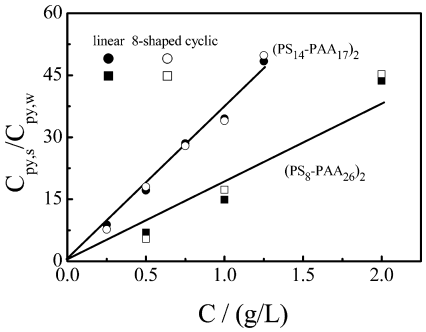

Figure 9. Amphiphilic copolymer concentration (C) dependence of relative concentration of solubilized pyrene in aqueous solutions, where $C_{py,s}$ and $C_{py,w}$ are concentrations of solubilized pyrene with and without copolymers, respectively.

without the addition of the amphiphilic copolymers, respectively, and $C_{py,s}$ was calculated using $A_{py,s} = \varepsilon b C_{py,s}$, with $A_{py,s}$, ε (~36 000 M^{-1} cm^{-1}), and b (= 1.0 cm) the absorbance of pyrene in the polymer solutions with the subtraction of the absorbance due to PS−PAA polymer, the molar extinction coefficient of pyrene in polymer solutions, and the sample cell thickness. The measurement of the extinction coefficient (ε) of pyrene in polymer solutions at a wavelength of 340 nm was detailed in the Supporting Information (Figure S8). A combination of Figures 8 and 9 reveals that the concentration of the solubilized pyrene linearly increases with the copolymer concentration, but there is no observable difference between each pair of linear- and cyclic-(PS−PAA) copolymers. On the other hand, a comparison of 8-shaped cyclic-$(PS_{14}-PAA_{17})_2$ and cyclic-$(PS_8-PAA_{26})_2$ with a similar overall degree of polymerization reveals that it is better to design an amphiphilic copolymer with a proper longer hydrophobic block and a shorter hydrophilic block but to maintain the overall degree of polymerization, i.e., keeping the consumption of comonomers or the cost constant.

CONCLUSION

The comparative study of the interchain association, the emulsifying efficiency, and the solubilization ability of two sets of well-defined amphiphilic linear-$(PS-PAA)_2$ chains and their 8-shaped cyclic-$(PS-PAA)_2$ counterparts with two rings reveals that both of the chain topology and the hydrophobic segment length can significantly affect their self-association in aqueous solutions and their emulsifying efficiency in the formation of polystyrene latex particles, but the chain topology has no observable effect on their solubilization capacity of hydrophobic pyrene. More specifically, in comparison with linear amphiphilic copolymers, those with an 8-shaped topology (i.e., two interconnected rings) self-associate less in water to form larger but looser aggregates because their hydrophobic segments are constrained inside each chain; provide no better emulsifying ability in the formation of polystyrene latex particles; and have a similar ability to solubilize hydrophobic pyrene in water. On the other hand, our results reveal that for a given overall degree of polymerization, it is better to properly increase the length of the hydrophobic segment in order to make these amphiphilic chains better emulsifying and dissolving agents. Our study also demonstrates that using these amphiphilic copolymers as interfacial stabilizers, we will have to consider both the interfacial surface area occupied by each copolymer chain and their anchoring ability at the interface; namely, one has to design a two-dimensional chain topology to cover a larger surface area for a given comonomer composition and at the same time incorporate a sufficiently long hydrophobic segment to ensure its insertion inside the stabilized phase. An umbrella- or mushroom-like topology with a large and flat hydrophilic top and some grafted hydrophobic blocks would be the best.

ASSOCIATED CONTENT

Supporting Information

Detailed experimental procedures of syntheses of initiator, linear- and 8-shaped cyclic-$(PS_8-PAA_{26})_2$, ^{1}H NMR spectra, ^{13}C NMR spectra, and Fourier transform infrared (FTIR) spectra of the intermediates in the preparation of the initiator, ^{1}H NMR spectra of linear-$(PS_{12}-PtBA_{13})_2$ before and after hydrolysis reaction, and characterization of polystyrene latex particles prepared by using amphiphilic linear- and 8-shaped cyclic-$(PS_8-PAA_{26})_2$ copolymers as emulsifiers. This material is available free of charge via the Internet at http://pubs.acs.org.

AUTHOR INFORMATION

Corresponding Authors

*E-mail llw@mail.ustc.edu.cn (L.L.).
*E-mail xdye@ustc.edu.cn (X.Y.).

Notes

The authors declare no competing financial interest.

ACKNOWLEDGMENTS

The financial support of the Ministry of Science and Technology of China Key Project (2012CB933800), the National Natural Scientific Foundation of China Projects (51173177 and 21274140), and the Hong Kong Special Administration Region Earmarked Projects (CUHK7/CRF/12G, 2390062; CUHK4036/11P, 2130281/2060431; and CUHK4035/12P, 2130306/4053005) is gratefully acknowledged.

REFERENCES

(1) Endo, K. *Adv. Polym. Sci.* **2008**, *217*, 121−183.
(2) Kricheldorf, H. R. *J. Polym. Sci., Part A: Polym. Chem.* **2010**, *48*, 251−284.
(3) Laurent, B. A.; Grayson, S. M. *Chem. Soc. Rev.* **2009**, *38*, 2202−2213.
(4) Qiu, X. P.; Tanaka, F.; Winnik, F. M. *Macromolecules* **2007**, *40*, 7069−7071.
(5) Su, H. H.; Chen, H. L.; Díaz, A.; Casas, M. T.; Puiggalí, J.; Hoskins, J. N.; Grayson, S. M.; Pérez, R. A.; Müller, A. J. *Polymer* **2013**, *54*, 846−859.
(6) Honda, S.; Yamamoto, T.; Tezuka, Y. *Nat. Commun.* **2013**, *4*, 1574.
(7) Touris, A.; Hadjichristidis, N. *Macromolecules* **2011**, *44*, 1969−1976.
(8) Takano, A.; Ohta, Y.; Masuoka, K.; Matsubara, K.; Nakano, T.; Hieno, A.; Itakura, M.; Takahashi, K.; Kinugasa, S.; Kawaguchi, D.; Takahashi, Y.; Matsushita, Y. *Macromolecules* **2012**, *45*, 369−373.
(9) Quirk, R. P.; Wang, S. F.; Foster, M. D.; Wesdemiotis, C.; Yol, A. M. *Macromolecules* **2011**, *44*, 7538−7545.
(10) Zhang, Y. N.; Wang, G. W.; Huang, J. L. *Macromolecules* **2010**, *43*, 10343−10347.
(11) Schulz, M.; Tanner, S.; Barqawi, H.; Binder, W. H. *J. Polym. Sci., Part A: Polym. Chem.* **2010**, *48*, 671−680.

(12) Lonsdale, D. E.; Bell, C. A.; Monteiro, M. J. *Macromolecules* **2010**, *43*, 3331−3339.
(13) Honda, S.; Yamamoto, T.; Tezuka, Y. *J. Am. Chem. Soc.* **2010**, *132*, 10251−10253.
(14) Misaka, H.; Kakuchi, R.; Zhang, C. H.; Sakai, R.; Satoh, T.; Kakuchi, T. *Macromolecules* **2009**, *42*, 5091−5096.
(15) Hu, J. W.; Zheng, R. H.; Wang, J.; Hong, L. Z.; Liu, G. J. *Macromolecules* **2009**, *42*, 4638−4645.
(16) Whittaker, M. R.; Goh, Y. K.; Gemici, H.; Legge, T. M.; Perrier, S.; Monteiro, M. J. *Macromolecules* **2006**, *39*, 9028−9034.
(17) Bielawski, C. W.; Benitez, D.; Grubbs, R. H. *Science* **2002**, *297*, 2041−2044.
(18) Gan, Y. D.; Dong, D. H.; Carlotti, S.; Hogen-Esch, T. E. *J. Am. Chem. Soc.* **2000**, *122*, 2130−2131.
(19) Ishizu, K.; Ichimura, A. *Polymer* **1998**, *39*, 6555−6558.
(20) Li, H. Y.; Riva, R.; Jérôme, R.; Lecomte, P. *Macromolecules* **2007**, *40*, 824−831.
(21) Oike, H.; Washizuka, M.; Tezuka, Y. *Macromol. Rapid Commun.* **2001**, *22*, 1128−1134.
(22) Kubo, M.; Hayashi, T.; Kobayashi, H.; Itoh, T. *Macromolecules* **1998**, *31*, 1053−1057.
(23) Li, H. Y.; Jérôme, R.; Lecomte, P. *Macromolecules* **2008**, *41*, 650−654.
(24) Jia, Z. F.; Fu, Q.; Huang, J. L. *Macromolecules* **2006**, *39*, 5190−5193.
(25) Fan, X. S.; Huang, B.; Wang, G. W.; Huang, J. L. *Macromolecules* **2012**, *45*, 3779−3786.
(26) Wang, G. W.; Fan, X. S.; Hu, B.; Zhang, Y. N.; Huang, J. L. *Macromol. Rapid Commun.* **2011**, *32*, 1658−1663.
(27) Shi, G. Y.; Sun, J. T.; Pan, C. Y. *Macromol. Chem. Phys.* **2011**, *212*, 1305−1315.
(28) Shi, G. Y.; Yang, L. P.; Pan, C. Y. *J. Polym. Sci., Part A: Polym. Chem.* **2008**, *46*, 6496−6508.
(29) Shi, G. Y.; Pan, C. Y. *Macromol. Rapid Commun.* **2008**, *29*, 1672−1678.
(30) Li, H. Y.; Riva, R.; Kricheldorf, H. R.; Jérôme, R.; Lecomte, P. *Chem.—Eur. J.* **2008**, *14*, 358−368.
(31) Tezuka, Y.; Komiya, R.; Washizuka, M. *Macromolecules* **2003**, *36*, 12−17.
(32) Oike, H.; Imaizumi, H.; Mouri, T.; Yoshioka, Y.; Uchibori, A.; Tezuka, Y. *J. Am. Chem. Soc.* **2000**, *122*, 9592−9599.
(33) Schappacher, M.; Deffieux, A. *Macromolecules* **1995**, *28*, 2629−2636.
(34) Clark, P. G.; Guidry, E. N.; Chan, W. Y.; Steinmetz, W. E.; Grubbs, R. H. *J. Am. Chem. Soc.* **2010**, *132*, 3405−3412.
(35) Dobrynin, A. V.; Rubinstein, M. *Prog. Polym. Sci.* **2005**, *30*, 1049−1118.
(36) Morishima, Y.; Itoh, Y.; Nozakura, S.; Ohno, T.; Kato, S. *Macromolecules* **1984**, *17*, 2264−2269.
(37) Greene, A. C.; Zhu, J. H.; Pochan, D. J.; Jia, X. Q.; Kiick, K. L. *Macromolecules* **2011**, *44*, 1942−1951.
(38) Konkolewicz, D.; Poon, C. K.; Gray-Weale, A.; Perrier, S. *Chem. Commun.* **2010**, *47*, 239−241.
(39) Gaillard, N.; Guyot, A.; Claverie, J. *J. Polym. Sci., Part A: Polym. Chem.* **2003**, *41*, 684−698.
(40) Burguière, C.; Chassenieux, C.; Charleux, B. *Polymer* **2003**, *44*, 509−518.
(41) Burguière, C.; Pascual, S.; Bui, C.; Vairon, J. P.; Charleux, B.; Davis, K. A.; Matyjaszewski, K.; Bétremieux, I. *Macromolecules* **2001**, *34*, 4439−4450.
(42) Li, L. W.; Zhou, J. F.; Wu, C. *Macromolecules* **2012**, *45*, 9391−9399.
(43) Li, L. W.; Yang, J. X.; Zhou, J. F. *Macromolecules* **2013**, *46*, 2808−2817.
(44) Berne, B. P.; Pecroa, R. *Dynamic Light Scattering*; Plenum Press: New York, 1976.
(45) Zimm, B. H. *J. Chem. Phys.* **1948**, *16*, 1099−1116.
(46) Wu, C.; Xia, K. Q. *Rev. Sci. Instrum.* **1994**, *65*, 587.
(47) Kwak, Y.; Matyjaszewski, K. *Polym. Int.* **2009**, *58*, 242−247.
(48) Jakubowski, W.; Kirci-Denizli, B.; Gil, R. R.; Matyjaszewski, K. *Macromol. Chem. Phys.* **2008**, *209*, 32−39.
(49) Tsarevsky, N. V.; Braunecker, W. A.; Matyjaszewski, K. *J. Organomet. Chem.* **2007**, *692*, 3212−3222.
(50) Datta, H.; Bhowmick, A. K.; Singha, N. K. *J. Polym. Sci., Part A: Polym. Chem.* **2007**, *45*, 1661−1669.
(51) Sinaga, A.; Hatton, T. A.; Tam, K. C. *Biomacromolecules* **2007**, *8*, 2801−2808.
(52) Green, T. W.; Wuts, P. G. M. *Protective Groups in Organic Synthesis*; Wiley-Interscience: New York, 1999; pp 372−381, 415−419, 728−731.
(53) Schömer, M.; Frey, H. *Macromolecules* **2012**, *45*, 3039−3046.
(54) Zhou, X. C.; Ye, X. D.; Zhang, G. Z. *J. Phys. Chem. B* **2007**, *111*, 5111−5115.
(55) Peng, K. Y.; Wang, S. W.; Lee, R. S. *J. Polym. Sci., Part A: Polym. Chem.* **2013**, *51*, 2769−2781.
(56) Zhou, Z. Y.; D'Emanuele, A.; Lennon, K.; Attwood, D. *Macromolecules* **2009**, *42*, 7936−7944.
(57) Kannaiyan, D.; Imae, T. *Langmuir* **2009**, *25*, 5282−5285.
(58) Vyhnalkova, R.; Eisenberg, A.; van de Ven, T. G. M. *J. Phys. Chem. B* **2008**, *112*, 8477−8485.
(59) Cho, S. Y.; Allcock, H. R. *Macromolecules* **2007**, *40*, 3115−3121.
(60) Teng, Y.; Morrison, M. E.; Munk, P.; Webber, S. E.; Procházka, K. *Macromolecules* **1998**, *31*, 3578−3587.
(61) Almgren, M.; Grieser, F.; Thomas, J. K. *J. Am. Chem. Soc.* **1979**, *101*, 279−291.
(62) Astafieva, I.; Zhong, X. F.; Eisenberg, A. *Macromolecules* **1993**, *26*, 7339−7352.
(63) Noda, T.; Hashidzume, A.; Morishima, Y. *Macromolecules* **2000**, *33*, 3694−3704.
(64) Vorobyova, O.; Yekta, A.; Winnik, M. A.; Lau, W. *Macromolecules* **1998**, *31*, 8998−9007.
(65) Yekta, A.; Duhamel, J.; Brochard, P.; Adiwidjaja, H.; Winnik, M. A. *Macromolecules* **1993**, *26*, 1829−1836.